Available online at www.sciencedirect.com
ScienceDirect
Progress in Natural Science 18 (2008) 401–404
Progress in Natural Science
www.elsevier.com/locate/pnsc

Photosensitized damage to telomere overhang and telomerase RNA by riboflavin

Yuxia Liu, Fuqiang Du, Weizhen Lin *, Tiecheng Tu, Wenxin Li, Nianyun Lin

Key Laboratory of Nuclear Analysis Techniques, Shanghai Institute of Applied Physics, Chinese Academy of Sciences, Shanghai 201800, China

Received 28 June 2007; received in revised form 19 November 2007; accepted 3 December 2007

Abstract

By ESR spin elimination and photocleavage assay, the mechanisms of one-electron oxidation damage of oligonucleotides by excited triplet state of riboflavin (Rb) have been elucidated. The results demonstrate that Rb, an endogenous photosensitizer, is capable of cleaving single-stranded telomeric overhang and the template region of telomerase RNA under UVA irradiation, resulting in blocking of reverse transcription of telomeric DNA which leads to the apoptosis of cancer cells ultimately.

Keywords: Telomere; Telomerase; Riboflavin; ESR spin elimination; Excited triplet state

1. Introduction

Telomeres are special DNA–protein structures found at the ends of all vertebrates linear chromosomes [1]. Telomeric DNA in vertebrate consists of tandem repeats of guanine rich sequences (TTAGGG)*n*. Telomerase is a ribonucleoprotein enzyme that maintains telomere length by adding telomeric sequences onto chromosome ends. The RNA component of telomerase contains a template sequence responsible for synthesis of telomeric DNA and complete replication of chromosome ends [2,3]. The primary function of telomeres is to protect the ends of linear chromosomes from recombination, fusion and degradation [4]. Each replication of telomeric DNA results in 3′-end bases loose of telomeres in normal somatic cells as a consequence of that the ends of telomeric DNA cannot be completely replicated by DNA polymerase. This process eventually leads to critical shortening of telomeric DNA, which results in cell apoptosis or cell death. This is known as ''end replication problem'' and telomeres are called ''molecular clock'' thereby. In contrast to somatic cells, in 90% tumor cell telomerase becomes active and stabilizes the length of telomeres [5], leading to the immortality of cancer cells. Nowadays, telomeres and telomerase are of great research interest due to the special relationship between activity of telomerase and cancer cells.

Riboflavin (Rb) or vitamin B_2 widely exists in human organs and a variety of fruits in free and conjugated forms, where it plays significant roles in most important biological functions. Rb-induced one-electron oxidation of biomolecules can readily occur via Type I photosensitized oxidation [6] because of a high quantum yield of the excited triplet state of Rb ($^3Rb^*$) and a higher reduction potential [7], which further lead to the damage of biological target molecules. The results from *in vitro* and *in vivo* studies demonstrate that Rb is capable of inducing damage of cellular DNA, protein and other biomolecules via photosensitized oxidation process under the irradiation of UVA or visible light, resulting in cell death eventually.

Previous ESR spin elimination and laser photolysis studies revealed that $^3Rb^*$ can react with all nucleic acid bases via electron abstraction reaction at deaerated condition with a variety of reaction rates [6]. Therefore, Rb can

* Corresponding author. Tel.: +86 21 59554603; fax: +86 21 59553021.
E-mail address: linweizhen@sinap.ac.cn (W. Lin).

1002-0071/$ - see front matter
doi:10.1016/j.pnsc.2007.12.003

be recognized as a strong endogenous photosensitizer capable of photocleaving the single-stranded telomeric overhang and template region of telomerase RNA, inducing them to serious breakages of functional sequences which results in the death of cancer cells ultimately. Thus, we are aiming at developing a novel cancer phototherapeutic approach which is different from traditional photodynamic therapy (PDT) [8] of cancers.

2. Materials and methods

2.1. Detection of the reactivity of $^3Rb^*$ with a series of single-stranded telomeric sequence repeats by ESR spin elimination method

Rb-induced photosentized oxidation of single-stranded telomeric sequence repeats were detected on a Varian E-112 spectrometer (X band, 100 kHz field modulation, microwave power of 5 mW and modulation amplitude of 1.0 G) combined with spin-trapping methods [6].

2.2. Rb-induced photocleavage of ^{32}P-5′-end-labeled single-stranded telomeric sequence and the "DNA model" of template region of telomerase RNA

The oligonucleotides were ^{32}P-5′-end-labeled and purified according to the reported methods [9]. The samples to be irradiated contained ^{32}P-5′-$(TAGGGT)_4$ or ^{32}P-5′-CGTC TAACCCTAACTGAGAAGGC [3] (Takara, China), 60 μM Rb (Sigma) and sonicated calf thymus DNA in a total volume of 14 μl. The samples were irradiated at 365-nm wavelength at room temperature for 30 min. After irradiation, all reaction mixtures were ethanol-precipitated and dried, then redissolved in 1 M piperidine. After being heated at 90 °C for 30 min and quickly chilled on ice, all samples including the A + G and G-sequencing markers [10] were resuspended in denaturing gel-loading buffer and run on a 20% denaturing polyacrylamide gel and electrophoresed at 10 W for approximately 2 h. The sites of cleavaged bands were analyzed by autoradiography.

2.3. Rb-induced photocleavage of ^{32}P-5′-end-labeled template region of telomerase RNA

The methods for irradiation and treatment of samples were almost the same as the above-mentioned except that the telomerase RNA to be irradiated contained 200 μM Rb. After irradiation, the samples were treated with 1 M aniline acetate (Sigma), heated at 60 °C for 20 min (kept away from light) and quickly chilled on ice. The samples were ready for the next procedure.

2.4. Digestion of template region of telomerase RNA with RNase T1

The reaction mixture in a microtube contained ^{32}P-5′-RNA (Takara, China), 10 mg/ml tRNA, 1 U/μl RNase T1 (Sigma), 0.0012 g urea, 10 mM Na–citrate (pH 5.0) in a total volume of 8 μl. This reaction mixture was dissolved in the DEPC-treated deionized water, heated at 50 °C for 12 min, then additional 0.0022 g urea was added into it after the reaction mixture was chilled on ice.

2.5. Digestion of template region of telomerase RNA with alkaline hydrolysis

The reaction mixture contained ^{32}P-5′-RNA, 50 mM $Na_2CO_3/NaHCO_3$ (pH 9.0), 1 mM EDTA (pH 8.0), 0.25 mg/ml tRNA in a total volume of 30 μl. This reaction mixture was put in a 90 °C water bath for 15 min after being kept at 0 °C for 10 min, then quickly chilled on ice for the next procedure.

3. Results and discussion

3.1. Reactivities of $^3Rb^*$ with single-stranded telomeric sequence repeats

A stable free radical, 4-oxo-TEMPO, can capture $Rb^{-\cdot}$ produced from reactions of $^3Rb^*$ with nucleotides or DNA at room temperature. Thus, we can measure the yield of $Rb^{-\cdot}$ according to the percentage of diminution of 4-oxo-TEMPO and thereby determine the reactivities of $^3Rb^*$ with a series of single-stranded telomeric DNA [6,11–14], which exhibited that reactivities increase with the decrease of $D_{0.4}$ value. Fig. 1 and Table 1 demonstrate that the reactivities of the single-stranded telomeric DNA $(TAGGGT)n$ $(n = 1–5)$ increase with the increment of repeats (n). It is supposed that the ionization potential (IP) of single-stranded telomeric DNA decreases with the increment of repeats (n) due to stacked purine repeats $(AGGG)n$, which indicates a tendency of degressive IP similar to that of $(–G_n–)$ [15]. Evidently, it seems that there exists certain structural similarity between single-helical telomeric DNA and double-helical DNA. But the previous

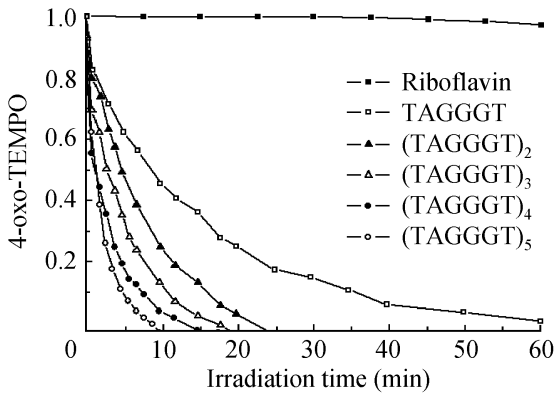

Fig. 1. Decrease of the ESR signal of 4-oxo-TEMPO aqueous solution during the irradiation. The samples contained 5 μM 4-oxo-TEMPO and 0.1 mM Rb, 1 mM $(TAGGGT)n$ $(n = 1–5)$. The samples were buffered with 10 mM sodium phosphate at pH 7.0, deaerated by high purity nitrogen and *in situ* irradiated by 365 nm light.

Table 1
Reactivity of (TAGGGT)n ($n = 1$–5) with $^3Rb^*$

	$D_{0.4}$ (J/cm^2)
TAGGGT	1.06
$(TAGGGT)_2$	0.64
$(TAGGGT)_3$	0.40
$(TAGGGT)_4$	0.21
$(TAGGGT)_5$	0.14

studies were mainly on double-helical DNA [16], not many on single-helical DNA, and the study for related IP is even less [17].

3.2. Photocleavage of the single-stranded telomeric DNA by $^3Rb^*$

A + G and G from Maxam–Gilbert sequencing reactions were used as markers for identification of Rb-induced photocleavage sites on the single-stranded telomeric DNA. Fig. 2 demonstrates that photocleavage sites are located at the AGGG sequence of all repeats (n) of (TAGGGT)n, whereas irradiated samples containing Rb but without piperidine treatment do not display a cleavage pattern. Our previous ESR spin elimination studies have identified the reactivities of $^3Rb^*$ with five nucleotides in the following order: dGMP > dAMP ≫ TMP ⩾ dUMP > dCMP. Moreover, theoretical and experimental results have indicated that IP of stacked contiguous GGG sequence is lower than that of G [15], that makes it susceptible to one-electron oxidation. As reported by Yoshioka et al. [17] the addition of cytosine (C) or thymine (T) to 5′ side of GGG in double-stranded DNA decreased the IP by 0.19 and 0.13 eV, respectively; thus CGGG and TGGG are deeper hole-traps than GGG. Evidently, in comparison with double-stranded DNA, AGGG in the single-helical telomeric DNA should be a deeper hole-trap due to stacked contiguous purines, which is capable of trapping hole transported via π-electron cloud as shown by the photodamage of AGGG in Fig. 2.

Alkaline hydrolysis of radical cation produced from reaction of $^3Rb^*$ with bases results in the scission of DNA-chain ultimately. The difference in IPs of G and A causes predominately the difference in yield of damaged base.

3.3. Photocleavage of template region of telomerase RNA by $^3Rb^*$

For consideration of the influence from experimental environment on the stability of RNA, we used a "DNA model" with a sequence equivalent to the template region of telomerase RNA to simulate Rb-induced photosensitized damage to the template region of telomerase RNA. Fig. 3 shows that every G in "DNA model" has been cleaved, which reveals that isolated G with low IP is susceptible to one-electron oxidation. In addition, we did not find the Rb-induced selective cleavage site at 5′G of GG in duplex DNA and this is contrary to the result reported by Saito et al. [18] that pyrimidine–G–pyrimidine sequences in duplex DNA are almost unreactive, but is

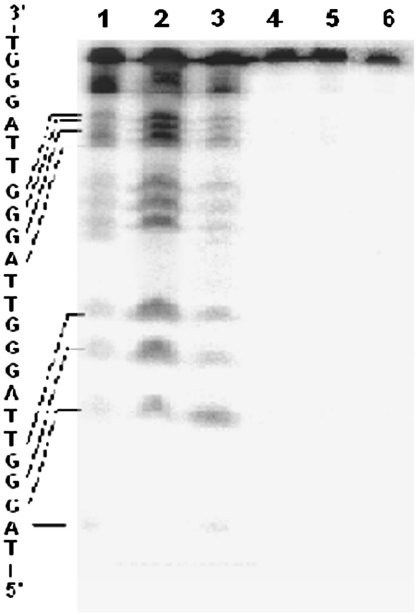

Fig. 2. Gel electrophoresis pattern of the Rb-induced photosensitized damage to single-stranded telomeric DNA. Lanes 1 and 2, Maxam–Gilbert sequencing reactions: A + G and G, respectively; lane 3, irradiation of DNA for 30 min in the presence of 60 μM Rb and with 1 M piperidine treatment; lane 4, the same as 3, no piperidine treatment; lane 5, irradiation of DNA without Rb, treated with piperidine; lane 6, DNA control, without piperidine treatment.

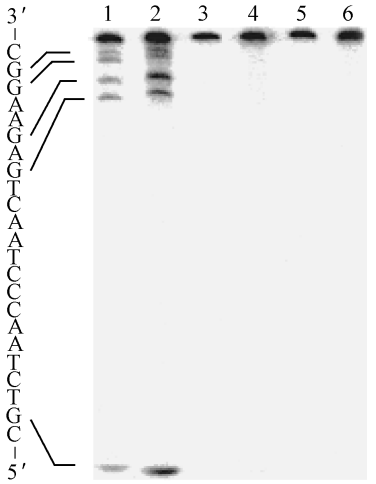

Fig. 3. Rb-induced photosensitized damage to the simulated template region of telomerase RNA. Lane 1, Maxam–Gilbert sequencing reaction G; lane 2, irradiation of DNA for 30 min in the presence of 60 μM Rb and 1 M piperidine treatment; lane 3, the same as 2, but without piperidine treatment; lane 4, irradiated DNA without Rb, treated with piperidine; lane 5, irradiation of DNA for 30 min; lane 6, DNA control, without piperidine treatment.

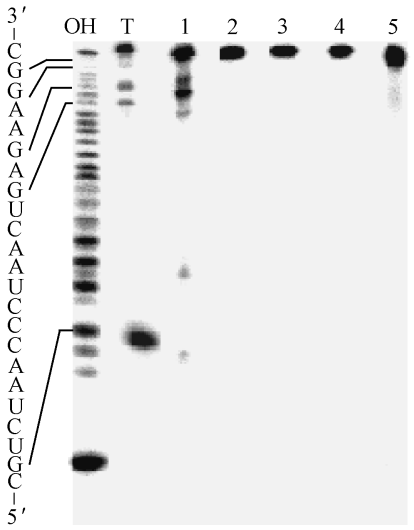

Fig. 4. Rb-induced photosensitized damage to the template region of telomerase RNA. OH, alkaline hydrolysis ladder; T, RNase T1-sequencing ladder; lane 1, irradiation of RNA for 30 min in the presence of 200 μM Rb, 1 M aniline acetate treatment; lane 2, the same as 1, but without aniline acetate treatment; lane 3, irradiated RNA without Rb, treated with aniline acetate; lane 4, irradiation of RNA for 30 min; lane 5, RNA control, without aniline acetate treatment.

consistent with that reported by Kan and Schuster [19] that isolated Gs are as reactive as GG in single-stranded DNA. Thus we infer that the structural difference between single- and double-stranded DNA exerts greater influence on reaction mechanisms for Rb-induced photosensitized damage to DNA in solution. Similarly, the results on the template region of telomerase RNA indicated that photocleavage mainly occurred at all Gs (Fig. 4). Moreover, a relative strong cleavage at 3′ side of template region might have provided an important target for cancer phototherapy. This is because of that once photocleavage-induced breakage at 3′ side of the template region occurring, the 5′ side of template region responsible for synthesis of telomeric DNA should never have any biological significance, it will result in inhibition of the function for reverse transcriptive synthesis of telomeric DNA ultimately.

4. Conclusions

Our findings proved that Rb can effectively induce widespread photocleavage of all the AGGG sequences in single-stranded telomeric DNA, this results in the loss of its function to keep the stability of chromosomes. Meanwhile, template region of telomerase RNA could also be photocleaved at all Gs. Evidently, this simultaneous cleavage of single-stranded telomeric overhang and telomerase RNA should inhibit formation of the hybrid duplex (DNA/RNA) which thereby blocks the reverse transcription for maintaining the length of telomeric DNA, and finally leads to apoptosis of cancer cells.

Acknowledgments

This work was supported by National Natural Science Foundation of China (Grant No. 20133020) and the Photo Science and Technology Research Foundation of Science and Technology Committee (022261014) of Shanghai, China.

References

[1] Rezler EM, Bearss DJ, Hurley LH. Telomeres and telomerases as drug targets. Curr Opin Pharmacol 2002;2:415–23.
[2] Blackburn EH. Telomerase. Annu Rev Biochem 1992;61:113–29.
[3] Chen JL, Blasco MA, Greider CW. Secondary structure of vertebrate telomerase RNA. Cell 2000;100:503–14.
[4] Neidle S, Harrison JR, Reszka AP, et al. Structure–activity relations among guanine-quadruplex telomerase inhibitors. Pharmacol Ther 2000;85:133–9.
[5] Shay JW, Bacchetti S. A survey of telomerase activity in human cancer. Eur J Cancer 1997;33:787–91.
[6] Lin WZ, Lu CY, Du FQ, et al. Reaction mechanism of riboflavin triplet state with nucleic acid bases. Photochem Photobiol Sci 2006;5:422–5.
[7] Hellis PF. The photophysical and photochemical properties of flavins (isoalloxazin). Chem Soc Rev 1982;11:15–39.
[8] Zheng XL, Jin YZ, Shen Y. Sensitizing drugs for cancer therapy. Shanghai: Science and Technology Literature Press; 2002, p. 254–65 [in Chinese].
[9] Yamamoto K, Kawanishi S. Site-specific DNA damage induced by hydrazine in the presence of manganese and copper ions. The role of hydroxyl radical and hydrogen atom. J Biol Chem 1991;266:1509–15.
[10] Maxam AM, Gilbert W. Sequencing end-labeled DNA with base-specific chemical cleavages. Methods Enzymol 1980;65:499–560.
[11] Pan JX, Liu Y, Zhang SP, et al. Photodynamic action of actinomycine D: an EPR spin trapping study. Biochim Biophys Acta 2001;1527:1–3.
[12] Moan J. A new method to detect porphyrin radicals in aqueous solutions. Acta Chem Scand 1980;B34:519–21.
[13] Reszka K, Sealy RC. Photooxidation of 3,4-dehydroxyphenylalanine by hematoporpyrin in aqueous solution: an electron spin resonance study using 2,2,6,6-tetramethyl-4-piperidone-1-oxyl (TEMPONE). Photochem Photobiol 1984;39:293–9.
[14] Hadjur C, Wagnieres G, Monnier P, et al. EPR and spectrophotometric studies of free radicals ($O_2^{-\cdot}$, OH, BPD-$MA^{-\cdot}$) and singlet oxygen ($^1O_2$) generated by irradiation of henzoporphyrin derivative monoacid ring A. Photochem Photobiol 1997;65:818–27.
[15] Sugiyama H, Saito I. Theoretical studies of GG-specific photocleavage of DNA via electron transfer: significant lowering of ionization potential and 5′-localization of HOMO of stacked GG bases in B-form DNA. J Am Chem Soc 1996;118:7063–8.
[16] Saenger W. Principles of nucleic acid structure. New York: Springer; 1984, p. 298–320.
[17] Yoshioka Y, Kitagawa Y, Takano Y, et al. Experimental and theoretical studies on the selectivity of GGG triplets toward one-electron oxidation in B-form DNA. J Am Chem Soc 1999;121:8712–9.
[18] Saito I, Nakamura T, Nakatani K, et al. Mapping of the hot spots for DNA damage by one-electron oxidation: efficacy of GG doublets and GGG triplets as a trap in long-range hole migration. J Am Chem Soc 1998;120:12686–7.
[19] Kan YZ, Schuster GB. Long-range guanine damage in single-stranded DNA: charge transport through a duplex bridge and in a single-stranded overhang. J Am Chem Soc 1999;121:10857–64.